

Comparing alpine watershed attributes from LiDAR, Photogrammetric, and Contour-based Digital Elevation Models

Chris Hopkinson,^{1*} Masaki Hayashi² and Derek Peddle³

¹ Applied Geomatics Research Group, Centre of Geographic Sciences, 50 Elliot Rd. Lawrencetown, Nova Scotia, B0S 1M0

² Department of Geoscience, University of Calgary, Calgary Alberta T2N 1N4

³ Department of Geography, University of Lethbridge, 4401 University Drive West, Lethbridge, Alberta T1K 3M4

Abstract:

As part of an alpine hydrological study in the Canadian Rocky Mountains, three digital elevation model (DEM) data sets were obtained for the purpose of watershed characterization. The data sources were: (1) archived public access BC TRIM (Terrain Resource Information Management) 1 : 20 000 contour vectors; (2) stereo aerial photography DEM with a derived point spacing between 5 m and 20 m; (3) airborne LiDAR (light detection and ranging) with point spacing from 1 m to 4 m. GIS layers of terrain and watershed attributes were created for each of the three DEM data sets at grid cell resolutions of 5 m and 25 m. Watershed attributes investigated were: DEM elevation, area, hypsometry, and stream network topology. In areas of lower relief and forest cover, the TRIM contour DEM contained topological errors at both 5 m and 25 m resolutions due to the poor representation of terrain from widely spaced contours. The photo DEM introduced obvious stream topology errors at 25 m due to the inability of the photo DEM to discern subtle terrain beneath forest canopies. The photo and TRIM DEMs overestimated basin hypsometry relative to the LiDAR watersheds at highest elevations due, in part, to their inability to represent the inside of gullies and steps associated with geological strata. In the case of the photo DEM, selectively digitizing break lines such as cliff edges, while missing shadowed areas, led to the creation of an interpolated surface that was biased towards the outer extremities of the terrain. Conversely, relative to the photo-based datasets, the LiDAR DEM better captured the inside of gullies and steps while under-sampling break line features, leading to a bias in the interpolated surface towards internal terrain extremities. As would be expected, the quality and resolution of the terrain data increased from BC TRIM to photo to LiDAR. If modelling watersheds within the Canadian Rockies at the meso scale and above, BC TRIM (or equivalent) 1 : 20 000 contour vectors would be most appropriate given availability and cost considerations. The benefits of LiDAR are apparent if higher resolution and more accurate watershed attribute information is needed detailing first-order hydrological channel features on steep shadowed mountain slopes or zero-order hill-slope depressions beneath forest canopies. Such landscape features provide preferential storages for winter snowpack in mountainous watersheds, suggesting that in the future LiDAR might be a tool of choice for snowpack resource monitoring in these regions. Copyright © 2008 John Wiley & Sons, Ltd.

KEY WORDS DEM; alpine watershed; LiDAR; GIS

Received 20 December 2007; Accepted 20 August 2008

INTRODUCTION

With the growing availability of high resolution terrain and landcover image data that provide important hydrological and water resources information (Pietroniro and Leconte, 2005), GIS modelling approaches are becoming popular for runoff simulation tasks. Perhaps the most important of these data sources is the digital elevation model (DEM). DEMs enable the direct extraction of watershed attributes such as channel network topology, channel storages and watershed extent; while also providing critical data on terrain attributes that control the distribution of hydrometeorological inputs such as radiant energy, precipitation, and sensible heat. DEM data, therefore, allow one to distribute and model hydrological inputs, transfers and outputs both spatially and with

elevation. Given the reliance on DEM data for deriving watershed, flow routing and hydrometeorological parameters, it follows that DEM limitations could be propagated throughout hydrological model simulations (Wechsler, 2007).

Extracting accurate stream network information from DEMs tends to be challenging in relatively flat landscapes where subtle errors in relief can have a significant impact on local slope and the placement of channel segments (e.g. Lindsey and Creed, 2005a), and at lower resolutions where channel features can be effectively 'smoothed' over (e.g. Lindsey and Creed, 2005b). Further, the type of DEM used can have an impact on the extraction of watershed hydrological features. For example Creed *et al.* (2003) compared the ability to automatically extract wetland features from independent DEM data sources that were based on publicly available contour vectors, aerial photography and airborne LiDAR. Results differed markedly between DEM type suggesting that both the resolution of the raw data, and the method of DEM

*Correspondence to: Chris Hopkinson, Applied Geomatics Research Group, Centre of Geographic Sciences, 50 Elliot Rd. Lawrencetown, Nova Scotia, B0S 1M0. E-mail: chris.hopkinson@nscc.ca

acquisition and generation have a marked impact on the ability to extract features of hydrological significance.

The effect of scale and data resolution on terrain attribute extraction has been discussed by Band and Moore (1995), while a comparison of two popular DEM data sources (LiDAR and stereo photogrammetry) was provided by Baltasvias (1999a). This paper builds on the above studies by applying generic GIS watershed attribute extraction routines to three independent DEM data sources (stereo aerial photograph, LiDAR, and publicly available contour data) within an alpine headwater environment. The comparison presented is original in that few studies have dealt with these three types of DEM sources, particularly in an area of challenging, high relief mountainous terrain and involving assessment of DEM sources with regard to subsequent derivation of hydrologically significant variables.

A benefit of LiDAR over other more traditional terrain data sources for the derivation of drainage networks is that it can be used to generate DEMs at resolutions approaching or better than 1 m point spacing. LiDAR therefore offers the potential to identify zero- (Tsukamoto *et al.*, 1982) and first- (Strahler, 1957) order drainage features (such as hill slope depressions and alpine gulleys) that control runoff generation and flow routing processes in headwater environments. Further, it can be used to map high resolution landscape depressions of hydrological importance even beneath forest canopies (Lindsey *et al.*, 2004), where traditional stereo photogrammetric methods tend to be weak due to canopy shadowing (Maune, 2001). However, the accuracy of LiDAR elevation data, and therefore hydrological features or indices associated with surface morphology, is influenced by data acquisition parameters (Hopkinson, 2007), terrain slope (Hodgson and Bresnahan, 2004) and vegetation cover (Bowen and Waltermire, 2002; Reutebuch *et al.*, 2003; Töyrä *et al.*, 2003; Hopkinson *et al.*, 2005). For a well calibrated LiDAR sensor collecting data over flat unambiguous surfaces, it is common to achieve root mean square errors (RMSE) in the elevation data below 15 cm (e.g. Hopkinson *et al.*, 2005; Hopkinson and Demuth, 2006). However, the magnitude of observed RMSE values may reach 30 cm or more on steeper slopes and densely vegetated surfaces.

The analysis presented in this paper was performed as part of a hydrological study of the glaciated watershed of Lake O'Hara in the Canadian Rocky Mountains (see Study area below), in which the delineation of small-scale features is very important for understanding the spatial variability of hydrological processes, such as snow accumulation and melt, runoff generation, and surface and subsurface storage of water. The recent retreat of mountain glaciers (Young, 1991; Hopkinson and Young, 1998; Demuth and Pietroniro, 2003; Hopkinson and Demuth, 2006) and the predicted shift in peak snow melt to earlier in the year (Pietroniro *et al.*, 2007) coupled with potentially warmer future climates has created considerable concern in Alberta and other downstream prairie provinces that rely on Rocky Mountain river flows for

water supplies. Therefore, from a resource-management perspective, there is a need to better understand hydrological processes and improve our hydrological models in alpine regions.

Recently, airborne LiDAR data has been demonstrated as an effective tool to map alpine environments at high accuracy and high resolution (Kennet and Eiken, 1997; Hopkinson *et al.*, 2001; Favey *et al.*, 2002; Arnold *et al.*, 2006). The challenge of obtaining accurate photogrammetric elevation estimates in snow covered areas of minimal surface texture, low contrast and high reflectance is overcome by the active nature of the LiDAR sensor (Favey *et al.*, 1999); however, limited horizontal accuracy leads to reduced elevation accuracy in areas of steep slopes or crevasses (Favey *et al.*, 2000; Hopkinson and Demuth, 2006), with break lines (such as cliffs edges) being particularly problematic due to the low probability of actually sampling the position of the edge (Smith *et al.*, 2004). In areas of high relief, small horizontal errors can propagate into large vertical elevation errors (Hodgson *et al.*, 2005; Hopkinson and Demuth, 2006). Thus, there is a need to assess the accuracy of LiDAR data in comparison to other data sources in the steep alpine terrain.

The objectives of the study are: (i) to investigate the influence DEM data source has on watershed parameter extraction; and (ii) to assess whether or not the watershed parameter information content for each DEM was consistent between two different grid resolutions. Specifically, three DEM data sources are compared: (i) publicly available 1:20 000 scale British Columbia government Terrain Resources Information Management (BC TRIM) GIS elevation data layers; (ii) a DEM derived from stereo aerial photography specifically acquired for hydrological research; and (iii) an airborne LiDAR derived DEM. For each of these data sources, raster DEMs were derived at 5 m and 25 m grid resolutions. These resolutions were chosen as 5 m was the highest that was reasonably achievable for all three data sources, while 25 m was considered more typical for larger area and regional studies due to its similarity to land cover data layers derived from satellite products (e.g. Landsat) and USGS 7.5 min DEM data sources. In addition, 5 m resolution DEMs take up 25 times more storage capacity than 25 m grids, thus for large drainage basin areas this might not be a practical resolution to adopt, even if the data are available.

The watershed attributes compared were: (i) watershed extent and area; (ii) watershed elevation statistics and hypsometry; and (iii) stream channel network. To ensure the analyses presented are as widely applicable as possible, all watershed GIS operations were performed using the widely available and utilised Arc Hydro tools (Maidment, 2002) within the Arc GIS suite (ESRI, Redlands, California).

STUDY AREA

The Lake O'Hara watershed is located in Yoho National Park in the Canadian Rocky Mountains on the British

Columbia side of the continental divide (51.21°N, 116.19°W). The ~14 km² watershed encompasses rugged terrain and ranges in elevation from 2010 m to 3490 m a.s.l. (Figure 1). It is comprised of sedimentary bedrock, predominantly of thickly-bedded quartzite and quartzose sandstone separated by thin layers of siltstone, sandstone and grey shale, of the Cambrian Gog Group with carbonate rocks at the summit of most peaks (Price *et al.*, 1980; Lickorish and Simony, 1995). Approximately 20% of the watershed is sub-alpine coniferous forest and 80% is alpine. The alpine terrain consists of exposed bedrock (40%), talus slopes (25%) and glacial moraine materials (15%) (Hood *et al.*, 2006). Local meteorological records indicate an annual total precipitation between 1100 mm and 1500 mm, depending on elevation. The watershed is snow-covered for about 8 months of the year and contains Opabin Glacier and several other small glaciers.

The Lake O'Hara watershed has been studied as a hydrological research basin equipped with a dense network of hydrometeorological and hydrometric monitoring stations. The rugged alpine terrain of the watershed exerts a dominant controlling influence on hydrological transfers and interactions. For example, accurate DEMs may be used to estimate the volume and spatial distribution of talus and moraine deposits, which control the subsurface water storage and pathways in the alpine environment (Clow *et al.*, 2003; Roy and Hayashi, 2008). Small-scale variability in slope angle and aspect has a critical influence on snow accumulation and melt (Winstral and Marks, 2002), which in turn affects the flow regime of mountain streams (Anderton *et al.*, 2002). High elevation gulleys act to store winter snowpack and retard melt late into the summer (Figure 2). DEMs, therefore, play an important role in both understanding the watershed processes and representing them within hydrological models. As a small heavily studied alpine watershed, the Lake O'Hara watershed provides an ideal location for the DEM attribute comparison that is the subject of this paper.

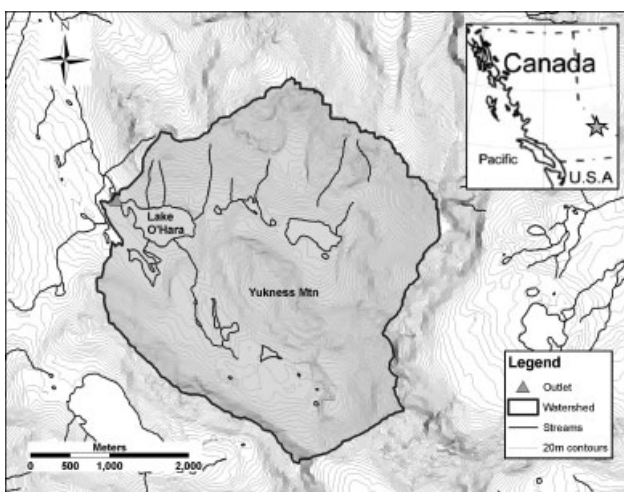


Figure 1. Lake O'Hara study watershed on the Alberta/BC border in the Canadian Rocky Mountains. Contour and Stream features are BC TRIM data layers



Figure 2. Oblique aerial photograph collected during the 2006 LiDAR survey illustrating the upper slopes of the watershed. Note the sharp ridges, steep bedrock slopes and numerous vertical gulleys in the rock faces

DEM ACQUISITION AND PRE-PROCESSING

BC Provincial Government TRIM DEM

British Columbia Terrain Resource Information Mapping (TRIM) contour data were obtained as a digital 1:20 000 map (Figure 3) in Arc GIS format from the Base Mapping and Geomatics Services Branch of the BC Ministry of Sustainable Resource Management (BC TRIM, 2006). All horizontal positional data were provided in the NAD 83 reference frame, with terrain heights relative to the GRS80 ellipsoid. Given the intent of the paper was to compare attributes directly derived from different DEM sources, we did not utilize the BC TRIM feature layers describing water courses and lakes within this analysis. From a cursory analysis of the BC TRIM water feature layer within the alpine study area it was found that the stream network was discontinuous and grossly over-simplified (see Figure 1), and would thus not provide any meaningful basis for comparison with derived stream network attributes.

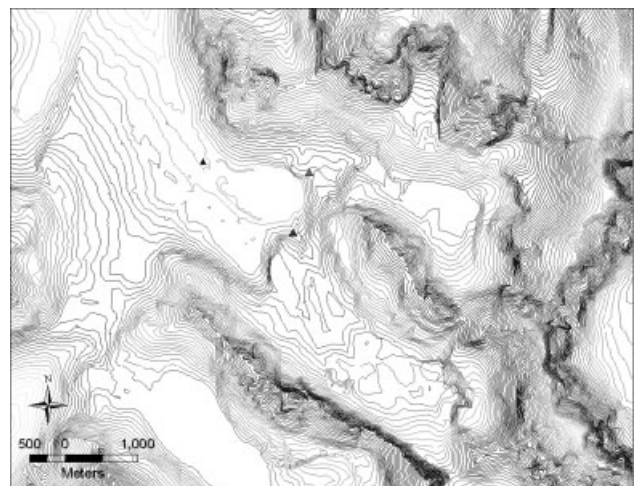


Figure 3. BC TRIM contour data around Lake O'Hara watershed

To facilitate comparable DEM data formats for subsequent watershed parameter extraction, all terrain datasets were converted to raster grids. The 1:20 000 BC TRIM contour data were converted to raster DEMs at 5 m and 25 m grid resolution using the Topo-to-Raster tool within ArcGIS v9.2 (ESRI, 2008). The default settings were applied. The Topo-to-Raster interpolation method is the most widely available tool for the conversion of vector-based contour data to raster surfaces and was designed specifically for the creation of hydrologically correct DEMs. The method utilizes a discretized thin plate spline technique (Wahba, 1990) that emphasizes ridges and stream channels, and is based on the ANU-DEM program developed by Hutchinson (1989).

Photogrammetric DEM from stereo aerial photography

Black and white stereo aerial photography was collected over the study site on 28 August 2006 (Figure 4). Image acquisition and photogrammetric data processing were carried out by the private company Geodesy Remote Sensing (Okotoks, Alberta). The camera used was a Zeiss Jena LMK 15 with a Lamegon PI lens calibrated to a focal length of 152.05 mm and equipped with image motion compensation. Following image acquisition, the diapositives were mounted within a digital stereo photogrammetric workstation for extraction of point elevations. Elevation measurements were digitized at regular 5 m grid node intervals over approximately 75% of the watershed and at major break lines within the terrain (Figure 4). In the forested lower reaches of the watershed, the grid nodes were more irregular and less dense due to the ground surface being obscured by the overlying forest canopy. Slightly reduced grid spacing also occurred on steep slopes in the upper reaches of the watershed due to difficulty observing common features at regular grid spacing in complex gullied and shadow-prone terrain.

The photogrammetric point elevations were referenced to five rapid static GPS ground control points (GCPs) collected within the watershed prior to the mission

and registered to the NAD83 CSRS (Canadian Spatial Reference System) reference frame. The coordinates of the base station used for differential correction of the control points were derived using stand alone precise point positioning (NRCAN, 2004) with no differential correction due to the lack of suitable benchmark in the vicinity. Consequently, there could be a positional offset of a few metres between the photo, TRIM and LiDAR DEMs due to the use of different survey control methods. However, the relative coordinates of the five GCPs were accurate to within 0.1 m. The output point data were converted to 5 m and 25 m raster grids using an inverse distance weighted (IDW) interpolation algorithm with a second-order power and a search radius of 100 m (Golden Software Inc., 2002). The 5 m IDW grid procedure maintained the photogrammetric grid node positions over the approximately 75% of the watershed that had a regular grid of raw data points, while positions were interpolated to a higher resolution beneath the tree canopy and on the steep upper slopes. The 25 m IDW procedure effectively 'smoothed' the raw point data across the entire watershed.

Airborne LiDAR DEM

The airborne LiDAR survey was conducted within 1 week of the photo mission on 25 August 2006, and used an Optech Inc. (Toronto, Ontario) airborne laser terrain mapper (ALTM) model 3100. The survey was performed in early afternoon during partial cloud cover, thus limiting the aircraft flying altitude to between 500 m a.g.l. and 2000 m a.g.l. (depending on ground elevation). The ALTM emitted and received 33 000 pulses s^{-1} of infrared (1064 nm) laser light to record ranges from the aircraft platform to the ground. The pulse beam diameter was 0.3 mrad, meaning that at altitudes of 1000 m above ground, the pulse footprint was approximately 0.3 m across, while at 2000 m the footprint would be 0.6 m. The pulses were swept across the flight path at up to 20° either side of the trajectory to generate a swath of terrain

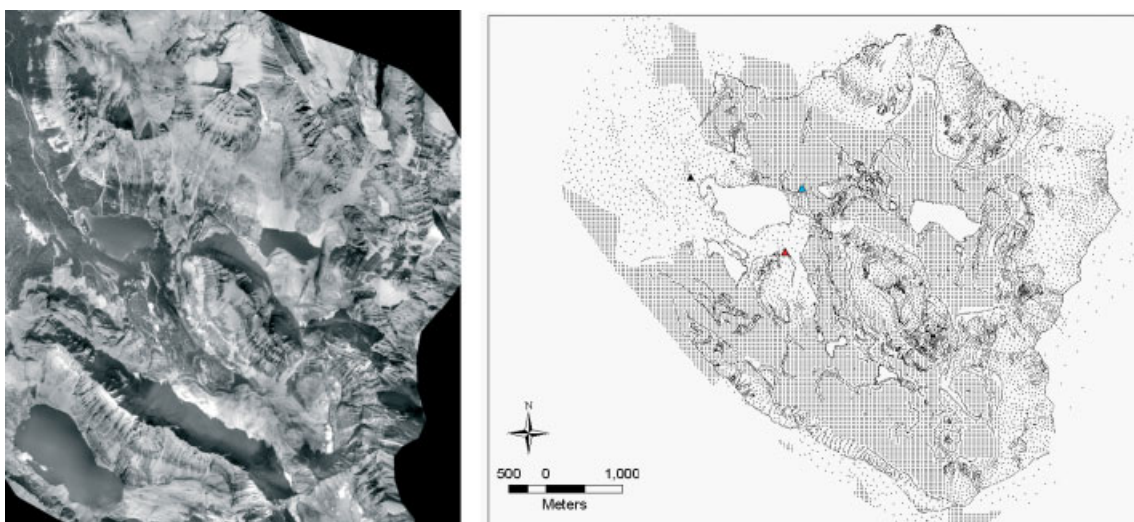


Figure 4. Air photo (left) and stereo softcopy derived terrain points at approximately 5 m postings (right). Note reduced point density on steep slopes in the upper reaches of the watershed and in forested areas in the lowest reaches

elevation data. The attitude of the aircraft was monitored 200 times each second using an inertial measurement unit (IMU). All data points were registered to a GPS receiver on the aircraft fuselage, which was differentially corrected to a GPS base station receiver set up over a survey monument on the Icefields Parkway 40 km north of survey area. The GPS trajectory, IMU, laser ranges, scan angle and calibration parameter data were post-processed in-house by the Applied Geomatics Research Group (Middleton, Nova Scotia) to generate ground point coordinates in the NAD83 CSRS reference frame. The horizontal spacing between adjacent LiDAR data points over the study area ranged from 1 m to 4 m.

To both calibrate the ALTM sensor and validate LiDAR coordinate positions, over 200 GPS points were collected along the length (1525 m) and width of Aidrie runway to the north of the airport of departure (Calgary International -YYC). A further 20 GPS points were collected around the perimeter of a small hangar roof at Aidrie airfield to validate horizontal point coordinate locations in both the along track and cross track directions of the flight path. The internal sensor component alignment was calibrated the day prior to the Lake O'Hara survey by collecting LiDAR data over the runway and the hangar roof. Angular misalignments were removed through a process of iterative angular adjustments until the LiDAR elevations and break line positions corresponded exactly with the ground surveyed positions. Three days following the survey, elevation (Z) was tested by flying six lines perpendicular to the runway and collecting full swaths of LiDAR data that could be directly compared to the GPS validation points. Validation of LiDAR coordinates in the along flight track direction (X) was performed by flying perpendicular to the hangar roof edge and collecting six profiles (0° scan angle) of points over the roof edge break line. Validation of LiDAR coordinates in the across flight track direction (Y) was performed by flying along the building edge and scanning a swath of points left and right across the roof edge break line. The comparison of LiDAR coordinates and GPS validation data was performed using Auto Calibrator (version 1.3.0-27) a proprietary software package developed by Optech Inc. For the elevation validation, all LiDAR points within a 0.5 m radius of a GPS point were compared and a summary of the statistics for each flight line provided. For the horizontal X and Y positional validation, Auto Calibrator filtered the LiDAR point data to identify the break line position at which the LiDAR scan or profile encounters the roof edge. The LiDAR break lines were then compared with the surveyed roof edge and the horizontal offsets calculated and summarized per flight line.

Following ALTM calibration and post-processing of the point output, the data collected over the forested lower reaches of the watershed were filtered in Terrascan (Terrasolid, Finland) to remove points floating above the ground surface. These ground classified LiDAR point data were combined with the points over the alpine areas and converted to 5 m and 25 m raster grids using an

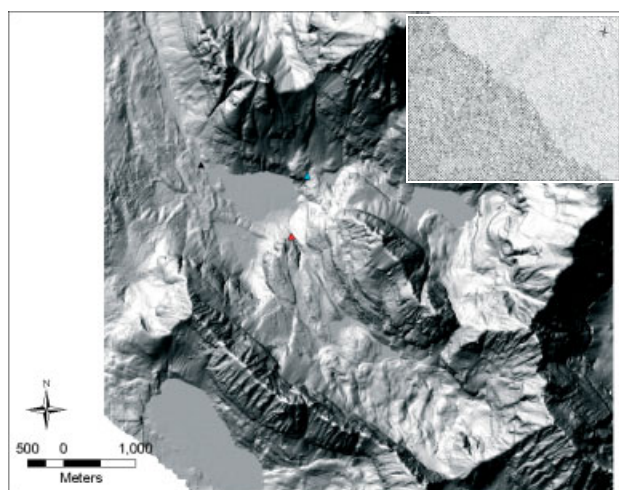


Figure 5. Shaded relief image of 5 m raster LiDAR DEM with illustration of raw LiDAR points (inset)

IDW interpolation algorithm (Golden Software, 2002) with a second-order power and a search radius of 100 m (Figure 5). The derived grid resolutions were both below that of the raw data, and so the interpolation procedure effectively smoothed or aggregated the LiDAR point data. Given the raw LiDAR were the most highly validated of the three data sources and the raw resolution is higher than the derived DEM grids, we consider the terrain information content within the LiDAR DEM to be generally the most reliable of the three methods. Therefore, the LiDAR derived DEMs will be used as the baselines for comparison.

WATERSHED ANALYSIS

After importing each of the raster DEM grids into an Arc GIS (ESRI, Redlands, California) project, each DEM was prepared to ensure equivalent spatial attributes. Where necessary, this involved transforming the grids to a common spatial reference frame (NAD83 horizontal, GRS80 vertical datums) and clipping the grids to a common area that extended beyond the bounds of the watershed. To ensure that this analysis would be relevant to the widest community possible, the extraction of watershed attributes was carried out using the Arc Hydro extension within Arc GIS (Maidment, 2002) as these tools are the most well known, accessible and widely utilized. For example, the United States Army Corps of Engineers (USACE) Hydraulic Engineering Center (HEC) hydrological (HMS) and hydraulic (RAS) modelling tools interface directly with the watershed attribute outputs from Arc GIS (Ackerman *et al.*, 2000; Brunner, 2006). Detailed descriptions of the algorithms and procedures are provided in Maidment and Djokic (2000) and Maidment (2002), and a review of these and alternative procedures is provided in Wechsler (2007).

Many of the Arc Hydro routines are built upon the simple deterministic eight node (D8) grid cell to grid cell flow direction algorithm of O'Callaghan and Mark

(1984), and Jensen and Domingue (1988). The authors recognize, however, that there are many more sophisticated and demonstrably accurate flow direction (Quinn *et al.*, 1991; Tarboten, 1997; Seibert and McGlynn, 2007) and depression filling (Martz and Garbrecht, 1998; Lindsey and Creed, 2005a, b) algorithms available. Unfortunately, none are as ubiquitous or straightforward to implement as those adopted in the Arc Hydro toolset. Given the purpose of this paper is to examine differences in watershed attributes due to DEM type and not to test algorithms, our approach is justified. However, we further recognize that some of the results of this analysis might differ if another suite of watershed attribute algorithms were used, and so the reader is cautioned to take this into account. A summary of the steps performed on each of the six DEMs is provided below and illustrated in Figure 6.

For the LiDAR and aerial photograph derived DEMs, the IDW interpolation algorithm left areas of blank nodes in regions where the search radius was too small to capture sufficient raw data from which to interpolate a grid node elevation. This occurred in areas of lakes and along the perimeter of the data acquisition area. To ensure these blank areas did not impact the hydrological attributes extracted from the DEMs, they had to be replaced with appropriate elevation values. This was achieved in two steps: (i) all blank nodes were replaced with temporary nodes containing elevations that were lower than their surroundings to introduce artificial sinks; (ii) a 'fill sinks' procedure (Band, 1986; Garbrecht and Martz, 2000) was performed on all DEM grids to ensure that there were no depressions in the DEM surface. A continuous DEM surface free from artificial depressions is a necessary requirement for the next step in the watershed attribute definition process: the extraction of 'flow direction'.

Arc Hydro utilizes the D8 flow direction algorithm (O'Callaghan and Mark, 1984; Jensen and Domingue, 1988) to ascertain the direction of surface runoff from the centre of any grid node to the centre of the lowest grid

node immediately adjacent to it. Following the creation of a flow direction layer, a flow accumulation procedure was performed to sum the total number of grid nodes that contribute runoff to each node in the DEM (Garbrecht and Martz, 2000). Nodes with a high flow accumulation value are most likely to lie on the stream network. Once a flow accumulation network was defined for each DEM, the watershed extent could be extracted using the 'watershed' tool in Arc Hydro. For this, the end point of the watershed must be defined so that the algorithm can work its way back up the flow accumulation network to the watershed boundary. The end point defined for this project was the outlet of Lake O'Hara. In Arc Hydro, the watershed outlet is referred to as a 'pour point'. The location of the pour point was manually defined but prior to being used in the watershed extraction process, was 'snapped' to the flow accumulation network associated with each individual DEM. For both the 5 m and 25 m DEMs, the start of the stream network was defined as a flow accumulation displaying a contribution area of at least 0.5 ha. This value was chosen based on several iterations and selecting the minimum contribution area that produced a stream network map that was visually neither too sparse nor too dense.

After the watershed attributes for each of the six DEMs had been extracted, comparisons were made between each DEM type and DEM resolution. For each DEM, summary statistics of the watershed elevations and areas were extracted, while the hypsometry, stream network topology and spatial extents of each extracted watershed were visibly compared. The spatial correspondence in watershed elevations was assessed by subtracting the TRIM and Photo DEMs from the LiDAR DEM.

RESULTS AND DISCUSSION

The results of the LiDAR calibration and validation missions collected prior to and following the actual data acquisition demonstrate that the ALTM sensor was

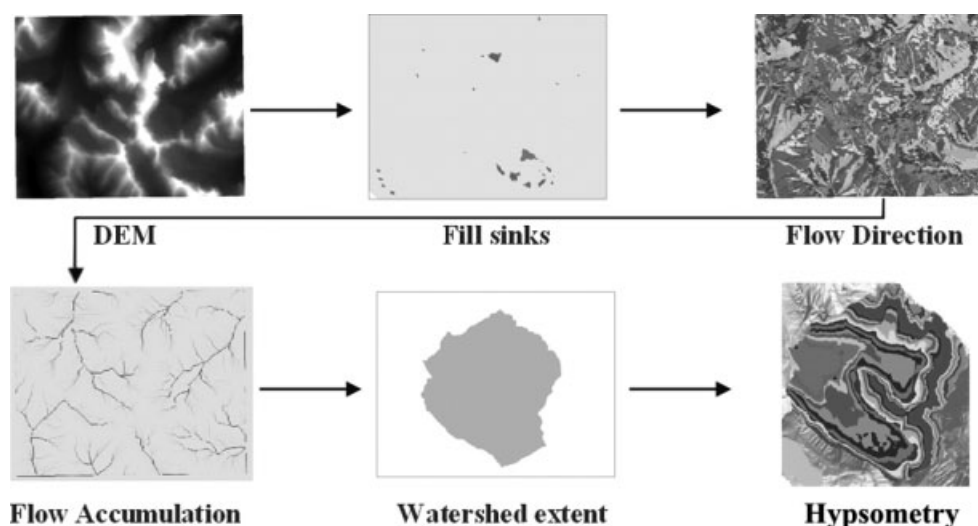


Figure 6. Schematic diagram illustrating processing sequence from DEM to watershed attribute layers

Table I. Horizontal and vertical LiDAR calibration and validation results for data collected over Airdrie airport runway and buildings prior to and following the Lake O'Hara data collection

Mission	Offset Statistic	Elevation (Z)	Along track (X)	Cross track (Y)
Calibration 24 th Aug	Average bias	−0.03m	−0.03m	0.00m
	RMSE	0.14m	0.10m	0.13m
	Sample size	232 points	12 edge crossings	112 edge crossings
Validation 29 th Aug	Average bias	−0.03m	0.32m	−0.18m
	RMSE	0.13m	0.36m	0.33m
	Sample size	>1000 points	12 edge crossings	>400 edge crossings

operating within the manufacturer specified tolerance of 0.15 m (Optech Inc., 2004) for flat surface elevations and 1 m (1/2000 the flying height) in the horizontal. A summary of the calibration and validation results is provided in Table I. No similar calibration or validation data are available for the aerial photograph or TRIM datasets.

Summary area and elevation statistics for the watersheds derived from each DEM are provided in Table II. The Lake O'Hara watershed area for the 5 m LiDAR DEM was 13.75 km², with elevations from 2010 m to 3395 m. The statistics for the 25 m LiDAR DEM are similar suggesting that the reduction in resolution had no appreciable impact on area or elevation range. This similarity in elevation properties is further evident when comparing the basin hypsometry for the 5 m and 25 m LiDAR DEMs (Figure 7). The slight reduction of 5 m in maximum elevation and overall range (Table II) might be expected due to the inevitable smoothing of narrow ridgelines (see Figure 2) within the higher reaches of the watershed when interpolating at lower resolutions. While the 5 m and 25 m LiDAR DEMs display similar area and elevation properties, the statistics for the aerial photograph and BC TRIM contour-based DEM watersheds demonstrate some notable differences (note: significance testing could not be performed due to there being only one of each watershed).

The area of the 5 m aerial photograph watershed was within 0.1 km² (or 1%) of the baseline LiDAR watershed, the 25 m photo DEM was 0.5 km² (or 3.5%) larger. Both the 5 m and 25 m BC TRIM watersheds were 2.2 km² (or 16%) larger. Minimum watershed elevations for both photo and TRIM DEMs were relatively close (from

Table II. Summary elevation statistics for each derived watershed

Statistics	LiDAR		Δ Photo		Δ TRIM	
	5 m	25 m	5 m	25 m	5 m	25 m
Area (km ²)	13.8	13.8	+0.1	+0.5	+2.2	+2.2
Min elevation (m)	2010	2010	+7	−13	+7	−9
Max elevation (m)	3395	3390	+50	+46	+32	+27
Mean elevation (m)	2500	2506	+27	+13	−24	−27
Elevation range (m)	1385	1380	+43	+59	+26	+36

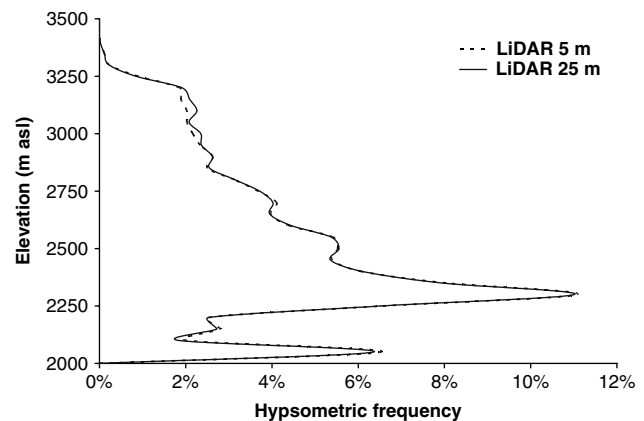


Figure 7. Watershed hypsometry for 5 m and 25 m LiDAR DEM

−13 m to +7 m) to that of the LiDAR DEM, while the maximum elevations displayed a larger positive deviation from +27 m to +50 m. For the air photo watersheds, this increase in maximum elevation corresponded with an increase in mean elevation of +27 m (5 m DEM) and +13 m (25 m DEM), while for the TRIM watershed, the opposite is true where the mean elevation was reduced by 24 m and 27 m for the 5 m and 25 m DEMs, respectively.

In the case of the 25 m photo watershed and both TRIM watersheds, these differences in elevation statistics can largely be explained by examining the spatial extents of the derived watersheds (Figure 8). From Figure 8, it is clear that for the 25 m DEMs most of the differences in the derived watershed boundaries occur near the watershed outlet. Results for the 5 m DEM (not shown) illustrate a similar pattern apart from a reduced difference between the LiDAR and photo watershed extents. There are slight deviations of up to 10 grid nodes at the edges of the watershed boundary at the upper reaches on the north, east and south sides of the watershed but >14% of the TRIM watershed and >3% of the photo watershed difference occurred near the watershed outlet on the west side (Figure 8). This suggests that the terrain information near the basin outlet within both the photo and TRIM DEMs was considerably different to the terrain information contained within the LiDAR DEM.

One of the major impacts of this increased watershed extent in the lower reaches of TRIM DEM is illustrated in Figure 9. In all three DEMs, the basin hypsometry illustrates greater area at the lower elevations between 2000 m

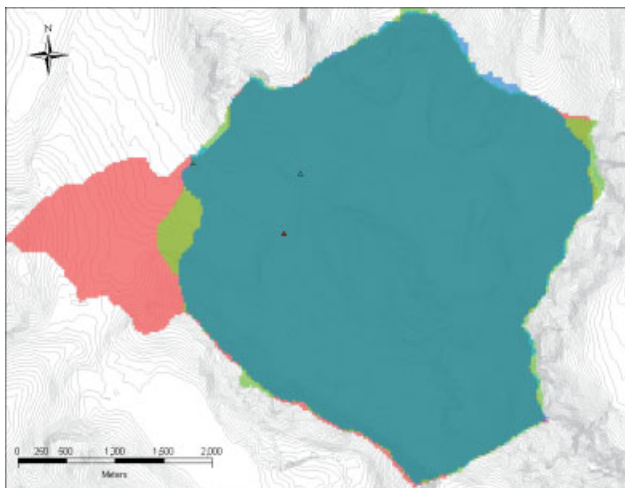


Figure 8. Watershed extents for LiDAR (blue), photo (green), and TRIM (red) 25 m DEMs

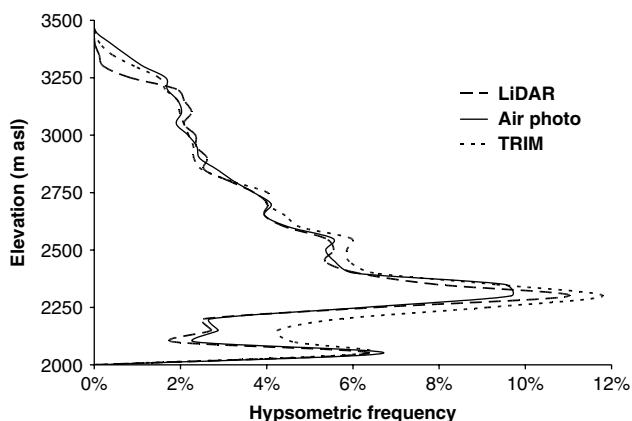


Figure 9. Watershed hypsometry for LiDAR, air photo and TRIM 25 m DEMs

and 2500 m. However, while the photo and LiDAR hypsometry is similar in this elevation range, the TRIM basin hypsometry demonstrates a systematic 1% to 3% increase in basin area throughout the 2100 m to 2600 m elevation range. Also of note is that at the upper reaches of the watershed (above 3250 m) both the photo and TRIM watersheds display a greater aerial coverage. This is consistent with the data in Table II, indicating that the LiDAR DEMs possess the lowest maximum elevation.

Less than 50% of the difference in high elevation basin area occurs around the edges of the watershed where deviations in extent between the DEM types are visible (Figure 8), thus suggesting some deviation in the position of ridgelines between DEM methods. However, the remaining contributing factor to the observation of reduced planar basin area in the upper region of the LiDAR DEM is due to the active (i.e. self-illumination) nature of this remote sensing technology. Rather than selectively sampling prominent and visible features in the landscape (as is the tendency with photogrammetric methods), it samples terrain according to an irregular grid of points. LiDAR data points sample inside high elevation gulleys and within the horizontal recesses of the

sedimentary bedding planes that give the upper mountain slopes their characteristic stepped profile (Figure 2). However, due to the non-selective method of elevation sampling, LiDAR data do not accurately capture break lines in the terrain (Maune, 2001; Hodgson *et al.*, 2003). This is because break line features rarely coincide exactly with LiDAR sampling location and so elevations are typically captured either side of the break line. During interpolation, therefore, ridge lines and terrace steps are artificially truncated, with the magnitude of truncation being a function of the LiDAR sampling density.

In both the photo and the contour-based TRIM (also originally derived from aerial photography) datasets, exterior terrain break lines (such as ridges) are systematically emphasized due to their visibility, while the inner recesses of gulleys and horizontal steps are rarely sampled due to being in shadow and invisible to passive photographic methods. Consequently, when interpolating raster DEMs from passive aerial photo-based or contour data, it is likely that systematic overestimation of the planar basin area in upper reaches will occur. Relative to photo-based methods, LiDAR data are better at capturing elevations within shadow areas while tending to sample either side of sharp ridges and cliff edges; therefore, it is likely that any bias in the LiDAR DEM would be to underestimate terrain area on high steep slopes. In the difference surface (Figure 10) between the 5 m LiDAR and the aerial photograph DEMs, the aerial photograph DEM appears to overlie the LiDAR DEM in many gully and foot of slope locations but the most prominent difference is observed over the ridge lines, where it is clear that the photo DEM better represents these sharp break line features.

Another potential cause for different basin hypsometry between DEM types could be due to warp or stretch in

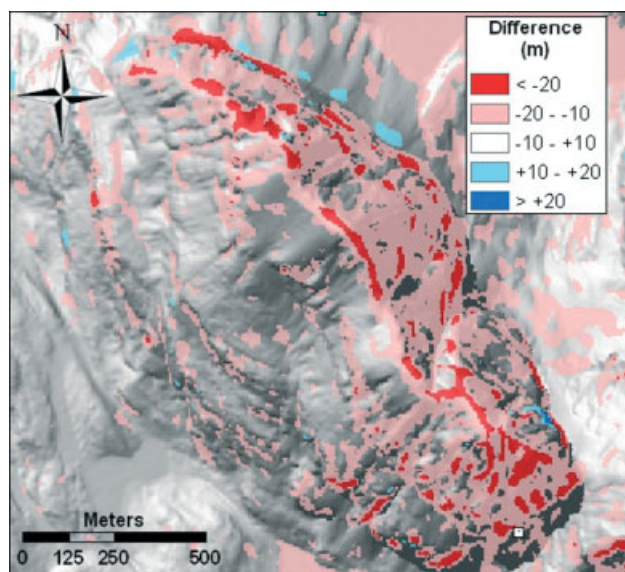


Figure 10. Elevation difference map overlaid onto shaded relief terrain image of Yukness Mountain in centre of Lake O'Hara watershed. A negative difference (red) illustrates that the photo DEM overlies the LiDAR DEM. Note most difference occurs along ridge lines and in gulleys

the raw data. With LiDAR data, if the sensor components are not correctly aligned it is possible for there to be systematic shifts in x, y or z, either in the whole dataset or between individual flight lines (Huising and Pereira, 1998). However, due to each LiDAR positional coordinate being the function of a highly calibrated active range and vector measurement from the aircraft platform, there is virtually no likelihood of a stretched DEM. Further, the calibration and validation data (Table I) demonstrate that the ALTM was operating well within specification for this mission. Stereo photogrammetric based DEMs, however, utilize the lens properties of the camera and GCPs to 'scale' the elevations within the digital elevation model (McGlone, 2004). Consequently, if the GCPs or the lens calibration parameters are inaccurate, this could propagate a scaling effect or stretch in the elevation data derived from the aerial photograph. It is not known how likely this might or might not be for the photo or TRIM datasets used in this study because only five GCPs were available. However, in the case of the photo DEM, all five GCPs were located within the lower 200 m elevation range of the watershed and so it is possible that small coordinate errors in one or more of the GCPs could propagate into a larger scaling error higher in the watershed.

Due to the dearth of reliable observational data detailing the position and topology of the actual stream network within the Lake O'Hara watershed, it was not possible to accurately validate the extracted stream network for each of the DEM types tested. As mentioned earlier, the TRIM water features layer was of some limited value but for the most part, this layer illustrated fragmented and minimal stream network detail within the confines of the Lake O'Hara watershed (Figure 1). However, from visual inspection the 5 m LiDAR stream network demonstrates a more 'natural' looking dendritic pattern (Figure 11), while the photo and TRIM watersheds display many parallel stream segments. This occurs, in part, because the photo and TRIM DEMs are derived from passive stereo imagery rather than the active illumination of light pulses, and thus small terrain depressions and channels are frequently in shadow and thus misrepresented or smoothed over. This reduction in terrain detail for an equivalent data resolution effectively creates a 'smoothed' DEM surface where the macro terrain features dominate the stream delineation process, thus leading to parallel stream channels. When the resolution in the LiDAR watershed was reduced to 25 m, the pattern still had a natural appearance, apart for the emergence of rectilinear stream-line artifacts typical of the D8 flow routing algorithm (Tarboten, 1997), and that the network was less extensive. This observation is consistent with the general reduction in terrain detail associated with lower resolution DEMs; i.e. true first-order stream channels are more likely to be 'smoothed' over at lower resolutions and therefore less visible or absent. However, despite the smoothing that occurs at lower resolutions, it is clear in Figure 11 that the most noticeable changes in stream channel topology

occur as a result of the different DEM methods from which the watershed is defined.

As with the lower resolution LiDAR DEM, the 5 m and 25 m photo and TRIM stream networks illustrated increased levels of rectilinear artifacts that clearly do not represent the natural stream network. Of note is that for the 25 m photo and both TRIM watersheds, the stream topology visibly deviated from that of the LiDAR DEM; this is most clearly illustrated in the vicinity of the watershed outlet (Figure 11). The photo DEM illustrates a tributary immediately upstream of the outlet entering from the south. From the TRIM water feature layer (and field observations), it is clear that this tributary actually enters the stream about 300 m down stream of the Lake O'Hara outlet (Figure 1). For both TRIM watersheds, this topological error is magnified further and led to the 15% increase in watershed extent on the west side that was reported in Table II and observed in Figure 8.

Apart from a resolution based simplification, the stream topology for the 5 m and 25 m LiDAR stream networks was similar and displayed no obvious deviations, suggesting that for the LiDAR DEM, a reduction in resolution does not seriously degrade the accuracy of the watershed or stream network attributes. For the photo DEMs, there are some deviations at the lower reaches of the watershed between the 5 m and 25 m DEMs, implying that the 5 m photo DEM is more accurate than the 25 m DEM. (Note: the convergence of network tributaries immediately upstream of the outlet in the 5 m photo DEM (Figure 11) occurs within the zero gradient environment of the lake (Figure 1) and thus the stream network topology in this area bears no resemblance to reality for any of the DEMs.) In both TRIM DEMs the stream network topology was compromised at both the 5 m and 25 m resolution, indicating that information contained in the 5 m TRIM DEM was probably not truly representative of this resolution; i.e. the 5 m TRIM DEM is likely no better than the 25 m DEM in terms of accurate watershed attribute information. Therefore, consistent with the observations of Band and Moore (1995) there is minimal benefit associated with the conversion of the 1:20 000 TRIM contour data to a higher resolution 5 m grid.

While data resolution no doubt plays a role, the observation that stream topology for the photo and TRIM watersheds is compromised near the basin outlet is also a function of the forest cover at the lower elevation ranges. Observing the ground surface and extracting accurate elevation data beneath forest canopies using passive aerial photography is challenging (Baltsavias, 1999a; Maune, 2001) and this is why the data point density in the forest area is low in the raw photo terrain dataset (Figure 4). The TRIM contour dataset was also ultimately derived from passive aerial photography and so suffers the same limitations. Another contributing factor to the erroneous stream network topology near the basin outlet was that the raw TRIM data represents the terrain with 20 m vertical contours. The area immediately surrounding the Lake O'Hara basin outlet has the lowest slope gradients of the entire watershed and thus the contours are widely spaced.

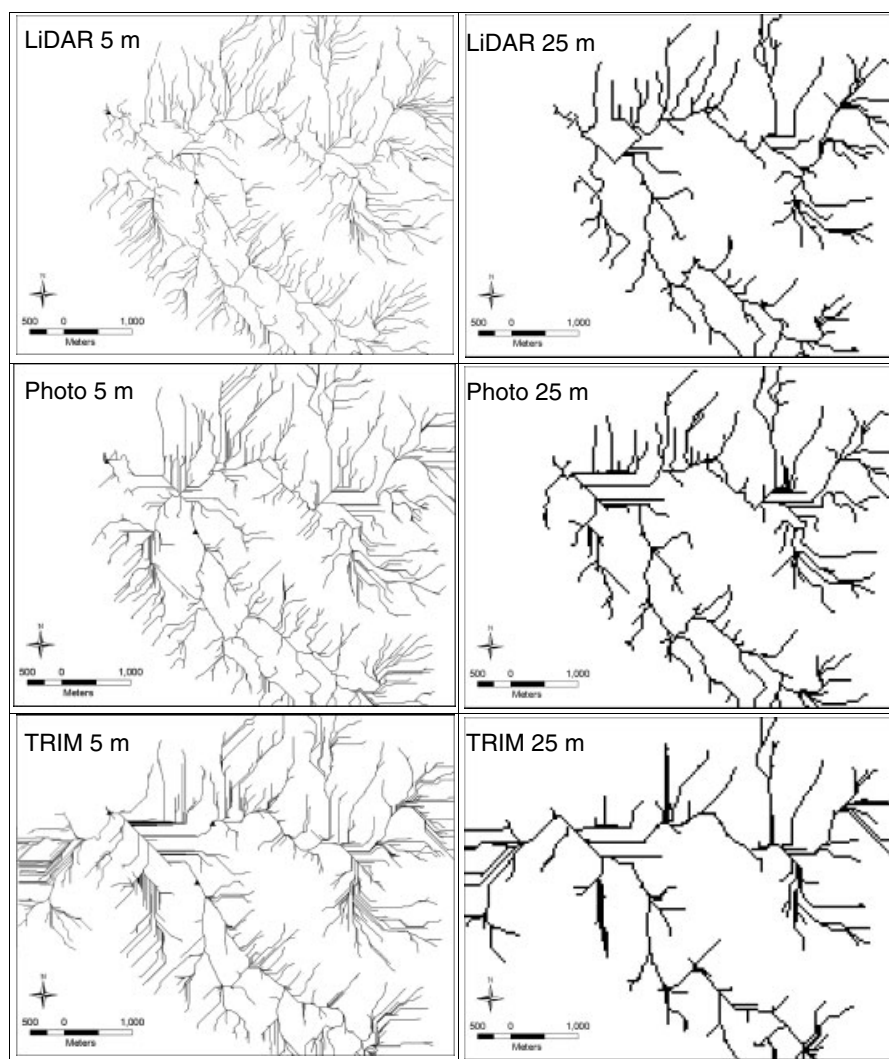


Figure 11. Derived watershed stream channel network for each DEM type

Therefore, even a small error in contour placement in a low gradient environment will result in erroneous drainage. LiDAR data, however, are derived from an active sensor that illuminates the ground beneath the canopy and can collect simultaneous returns from ground and canopy surfaces (Baltsavias, 1999b). Consequently, LiDAR can provide reasonably accurate terrain and surface drainage information even beneath forest canopy cover (Lindsey *et al.*, 2004).

CONCLUSIONS

This paper has addressed the lack of studies investigating different digital elevation model sources for GIS watershed attribute extraction in alpine environments. All three DEM types considered here demonstrated broad similarity in terms of basin attributes; however, there were important differences at finer scales and for particular application uses. The quality and resolution of the terrain data increased from BC TRIM to photo to LiDAR, as would be expected given TRIM data are the cheapest and easiest to acquire while LiDAR are the most costly

and difficult to acquire. If modelling watersheds within the Canadian Rockies at the meso-scale and above, any of the DEM types would suffice but the contour-based BC TRIM DEM data (or equivalent elsewhere) would likely be most appropriate given its availability in most jurisdictions and its lower cost. The benefits of commissioning dedicated photo and LiDAR missions can be justified if higher resolution and more accurate watershed attribute information are needed. For example, of the DEM sources considered here, the BC TRIM contour data do not adequately represent zero-order hillslope depressions beneath forest canopy or first-order channels within high elevation gulleys, whereas the LiDAR terrain data are best suited to this task.

Of particular interest from our results were the different levels of sensitivity found among the various DEM sources for the two different spatial resolutions tested (5 m, 25 m). The TRIM data had an inherently low resolution as well as associated topological issues that cannot be corrected internally. In areas of lower relief (typically at lower elevations in this study area), the TRIM DEM contained topological errors at both 5 m and 25 m resolutions due to the poor representation of

terrain from widely spaced contours. Although these data can be rasterised to any (artificially small) grid-size, the actual information content cannot be increased beyond the fundamental minimum mapping unit of the source data in those areas. The TRIM data were unacceptable for applications requiring actual 5 m source resolution, but were deemed appropriate at the 25 m grid-size for some hydrological parameters. The photo DEM was suitable in most situations at both 5 m and 25 m, although at 25 m some topological and extent errors were evident due to the inability of the photo DEM to discern subtle terrain beneath canopies at lower elevations. Some of these and other areas that contained terrain shadow were also problematic for the photo DEM due to the reduced level of discernment. This led to incorrect stream topology, an increase in basin area, and a slight upwards shift in basin hypsometry.

The best DEM source over the largest range of terrain was the LiDAR DEM. In areas of more complex terrain morphometry such as gullies that are important in alpine hydrological flow routing and storage processes, LiDAR provided the best characterization of the three DEM sources tested. The area, elevation range, hypsometry, and stream network topology for the 5 m and 25 m LiDAR DEM were similar, suggesting that the reduction in resolution had little appreciable impact on watershed attributes other than a smoothing of the terrain and the associated reduction in detail. This is indicative of a higher level of fundamental information content for this data source, from which fewer systematic errors were introduced when reducing the resolution (to 25 m in this case). However, the LiDAR did not perform as well compared to the photo DEM in capturing break line features such as ridges and cliff edges. These features are typically prominent in aerial photography due to the sharp visible contrast of shadow to non-shadow at break lines but are not captured to the same extent by LiDAR due to irregular point sampling of the terrain surface.

The photo and TRIM DEMs overestimated basin hypsometry relative to the LiDAR watersheds at highest elevations due, in part, to an inability of both DEM sources to accurately represent gullies and the interior recesses of bedrock steps associated with geological strata. In the case of the photo DEM, preferentially digitizing break lines while missing shadowed areas led to the creation of an interpolated surface that was biased towards the outer extremities of the terrain. Conversely, the LiDAR DEM better captured the insides of gullies and bedrock steps while under-sampling ridge line and cliff edge features, leading to an interpolated surface that was biased towards the internal extremities of the terrain. Differences such as these in watershed attributes due to DEM type could impact hydrometeorological parameter distributions and runoff predictions in hydrological models. For example, a downwards bias in basin hypsometry could slightly reduce total precipitation inputs or increase the rain to snow ratio and more importantly change the timing of snowmelt due to the influence of temperature lapse rates, thus altering the modelled hydrograph (Zappa

et al., 2003). This has possible implications for the prediction of stream flow for water resources management.

Beyond the central recommendation of LiDAR for producing DEMs for smaller area studies that require higher elevation accuracy in more complex terrain for hydrological parameters that justify its higher cost, we also note that of the three DEM sources tested, LiDAR also holds considerable further potential for technological gain and thus further improvements in products. Similar to the progression of other technologies, the community may expect the cost of LiDAR to stabilize and then become increasingly cost effective in parallel with increases in data coverage, technological advances, and adoption rates.

Given the point sampling pattern of LiDAR data, it is not necessarily the ideal tool for the accurate extraction of alpine terrain extremities such as along ridge lines and cliff edges. However, from a water balance and runoff generation perspective, such features play a relatively minor role compared to the preferential surficial flow paths and snowpack storages associated with gulleys and depressions. Therefore, given the increasing importance of snowpack water resources in mountainous headwater environments, and continued reductions in LiDAR acquisition costs, it is fair to speculate that LiDAR will gradually become a tool of choice for the assessment of winter snowpack resources in remote and heterogeneous alpine basins.

ACKNOWLEDGEMENTS

Dr Chris Hopkinson acknowledges infrastructure and operating funding from the Canada Foundation for Innovation (CFI), and funding from NSERC under the College and Community Innovation Program (CCIP). We thank Karen Miller for compiling the raw TRIM and photo DEM data layers and Jaime Hood for assisting with the aerial photo acquisition. The LiDAR data were collected through the *Canadian Consortium for LiDAR Environmental Applications Research* (C-CLEAR). This project was partially funded by the Alberta Ingenuity Centre for Water Research, G8 Legacy Chair in Wildlife Ecology, Environment Canada Science Horizons Program, and Canadian Foundation for Climate and Atmospheric Science through the *Improved Processes and Parameterization for Prediction in Cold Regions* (IP3) network. Mike Demuth of the Geological Survey of Canada is gratefully acknowledged for subsidizing the airborne lidar mission.

REFERENCES

- Ackerman CT, Evans TA, Brunner GW. 2000. HEC-GeoRAS: linking GIS to hydraulic analysis using ARC/INFO and HEC-RAS. In *Hydrologic and Hydraulic Modelling Support with Geographic Information Systems*, Maidment D, Djokic D (eds). ESRI Press: Redlands, CA.
- Anderton SP, White SM, Alvera B. 2002. Micro-scale spatial variability and the timing of snow melt runoff in a high mountain catchment. *Journal of Hydrology* **268**: 158–176.

- Arnold NS, Rees WG, Devereux BJ, Amable GS. 2006. Evaluating the potential of high-resolution airborne LiDAR data in glaciology. *International Journal of Remote Sensing* **27**: 1233–1251.
- Baltsavias EP. 1999a. A comparison between photogrammetry and laser scanning. *ISPRS Journal of Photogrammetry and Remote Sensing* **54**: 83–94.
- Baltsavias EP. 1999b. Airborne laser scanning: existing systems and firms and other resources. *ISPRS Journal of Photogrammetry and Remote Sensing* **54**: 164–198.
- Band L. 1986. Topographic partitioning of watersheds with digital elevation models. *Water Resources Research* **22**(1): 15–24.
- Band L, Moore I. 1995. Scale: landscape attributes and Geographical Information Systems. *Hydrological Processes* **9**: 401–422.
- BC TRIM. 2006. British Columbia Terrain Resource Information Mapping (TRIM) Digital Map Products. B.C. Ministry of Sustainable Resource Management, Base Mapping and Geomatics Services Branch. <http://srmwww.gov.bc.ca/gis/arctrim.html> [last accessed: Dec. 7, 2007].
- Bowen ZH, Waltermire RG. 2002. Evaluation of light detection and ranging (LiDAR) for measuring river corridor topography. *Journal of the American Water Resources Association* **38**: 33–41.
- Brunner G. 2006. *HEC-RAS, River Analysis System User's Manual*. Computer program documentation CPD-68. US Army Corps of Engineers, Institute for Water Resources, Hydraulic Engineering Center.
- Clow DW, Schrott L, Campbell DH, Torizzo A, Dornblaser M. 2003. Ground water occurrence and contributions to streamflow in an alpine catchment, Colorado Front Range. *Groundwater* **41**: 937–950.
- Creed IF, Sanford SE, Beall FD, Molot LA, Dillon PJ. 2003. Cryptic wetlands: Integrating hidden wetlands into models of dissolved organic carbon export. *Hydrological Processes* **17**: 3629–3648.
- Demuth MN, Pietroniro A. 2003. The impact of climate change on the glaciers of the Canadian Rocky Mountain eastern slopes and implications for water resource adaptation in the Canadian prairies—Phase I Headwaters of the North Saskatchewan River Basin. CCAF—Prairie Adaptation Research Collaborative, Study Report Project P55, plus Technical Appendices.
- ESRI. 2008. Environmental Systems Research Institute, ArcGIS v9.2 User's Manual. Redlands, California.
- Favey E, Cerniar M, Cocard M, Geiger A. 1999. Sensor attitude determination using GPS antenna array and INS. In *ISPRS WG III/I Workshop: Direct Versus Indirect Methods of Sensor Orientation*, Barcelona, 25–26 November; 28–38.
- Favey E, Pateraki M, Baltsavias EP, Bauder A, Bösch H. 2000. Surface modelling for alpine glacier monitoring by airborne laser scanning and digital photogrammetry. In *International Archives of Photogrammetry and Remote Sensing, XIXth ISPRS Congress*, Amsterdam: Vol. XXXIII (B4); 269–277.
- Favey E, Wehr A, Geiger A, Kahle HG. 2002. Some examples of European activities in airborne laser techniques and an application in glaciology. *Journal of Geodynamics* **34**: 347–355.
- Garbrecht J, Martz L. 2000. Digital elevation model issues in water resources modelling. In *Hydrologic and Hydraulic Modelling Support with Geographic Information Systems*. Maidment D, Djokic D (eds). ESRI Press: Redlands, CA.
- Golden Software Inc.. 2002. *Surfer® for Windows, version 8: user's guide*, Golden Software, Inc.: Colorado, USA.
- Hodgson ME, Bresnahan P. 2004. Accuracy of airborne lidar-derived elevation: empirical assessment and error budget. *Photogrammetric Engineering and Remote Sensing* **70**: 331–340.
- Hodgson ME, Schill S, Davis B, Jensen JR, Schmidt L. 2003. An evaluation of LiDAR- and IFSAR-derived digital elevation models in leaf-on conditions with USGS level 1 and level 2 DEMs. *Remote Sensing of Environment* **84**(2): 295–308.
- Hodgson ME, Jensen JR, Raber GT, Tullis JA, Davis B, Schuckman K, Thompson G. 2005. An evaluation of LiDAR-derived elevation and terrain slope in leaf-off conditions. *Photogrammetric Engineering & Remote Sensing* **71**(12): 817–823.
- Hood JL, Roy JW, Hayashi M. 2006. Importance of groundwater in the water balance of an alpine headwater lake. *Geophysical Research Letters* **33**: L13405, DOI: 10.1029/2006GL026611.
- Hopkinson C. 2007. The influence of flying altitude and beam divergence on canopy penetration and laser pulse return distribution characteristics. *Canadian Journal of Remote Sensing* **33**(4): 312–324.
- Hopkinson C, Demuth MN. 2006. Using airborne LiDAR to assess the influence of glacier downwasting to water resources in the Canadian Rocky Mountains. *Canadian Journal of Remote Sensing* **32**(2): 212–222.
- Hopkinson C, Young GJ. 1998. The effect of glacier wastage on the flow of the Bow River. *Hydrological Processes* **12**: 1745–1763.
- Hopkinson C, Demuth M, Sitar M, Chasmer L. 2001. Applications of LiDAR mapping in a glacierised mountainous terrain. *Proceedings of the International Geoscience and Remote Sensing Symposium*, Sydney, Australia. 9–14 July. Published on CDROM.
- Hopkinson C, Chasmer LE, Zsigovics G, Creed I, Sitar M, Kalbfleisch W, Treitz P. 2005. Vegetation class dependent errors in LiDAR ground elevation and canopy height estimates in a Boreal wetland environment. *Canadian Journal of Remote Sensing* **31**(2): 191–206.
- Huising EJ, Pereira LM. 1998. Errors and accuracy assessment of laser data acquired by various laser scanning systems for topographic applications. *ISPRS Journal of Photogrammetry and Remote Sensing* **53**(5): 245–261.
- Hutchinson MF. 1989. A new procedure for gridding elevation and stream line data with automatic removal of spurious pits. *Journal of Hydrology* **106**: 211–232.
- Jensen SK, Domingue JO. 1988. Extracting topographic structure from digital elevation data for geographic information system analysis. *Photogrammetric Engineering and Remote Sensing* **54**(11): 1593–1600.
- Kennet M, Eiken T. 1997. Airborne measurement of glacier surface elevation by scanning laser altimeter. *Annals of Glaciology* **24**: 235–238.
- Lickorish WH, Simony PS. 1995. Evidence for late rifting of the Cordilleran margin outlined by stratigraphic division of the Lower Cambrian Gog Group, Rocky Mountain Main Ranges, British Columbia and Alberta. *Journal of Earth Sciences* **32**: 860–874.
- Lindsay JB, Creed IF. 2005a. Removal of artifact depressions from digital elevation models: towards a minimum impact approach. *Hydrological Processes* **19**: 3113–3126.
- Lindsay JB, Creed IF. 2005b. Sensitivity of digital landscapes to artifact depressions in remotely-sensed DEMs. *Photogrammetric Engineering and Remote Sensing* **71**: 1029–1036.
- Lindsay JB, Creed IF, Beall FD. 2004. Drainage basin morphometrics for depressional landscapes. *Water Resources Research* **40**: W09307, DOI: 10.1029/2004WR003322.
- Maidment D. (ed). 2002. *Arc Hydro: GIS for Water Resources*. ESRI Press: Redlands, CA.
- Maidment D, Djokic D (eds). 2000. *Hydrologic and Hydraulic Modelling Support with Geographic Information Systems*. ESRI Press: Redlands, CA.
- Martz LW, Garbrecht J. 1998. The treatment of flat areas and depressions in automated drainage analysis of raster digital elevation models. *Hydrological Processes* **12**: 843–855.
- Maune DF (ed). 2001. *Digital Elevation Model Technologies and Applications: The DEM Users Manual*. American Society for Photogrammetry and Remote Sensing: Bethesda, ML.
- NRCAN. 2004. *Online Precise Point Positioning 'How To Use' Document; ver 1.1*. Natural Resources Canada, Geodetic Survey Division, Government of Canada, Ottawa. 25 pp. Online at <http://www.geod.nrcan.gc.ca/userguide/howtouse.pdf> [last accessed: Dec. 18, 2007].
- O'Callaghan JF, Mark DM. 1984. The extraction of drainage networks from digital elevation data. *Computer Vision, Graphics, and Image Processing* **28**: 328–344.
- Optech Incorporated. 2004. *ALTM 3100 specifications*. Optech Incorporated: Toronto, Ont.
- Pietroniro A, Leconte R. 2005. A review of Canadian remote sensing and hydrology, 1999–2003. *Hydrological Processes* **19**: 285–301.
- Pietroniro A, Demuth MN, Dornes P, Toyra J, Kouwen N, Ringeman A, Hopkinson C, Burn D, Brua B. 2007. Streamflow shifts resulting from past and future glacier fluctuations in the in the eastern flowing basins of the Rocky Mountains. Report to the Climate Change Research Users Group of the Government of Alberta, Alberta Environmental Protection.
- Price RA, Cook DG, Aitken JD, Mountjoy EW. 1980. *Geology, Lake Louise, Alberta and British Columbia, Map 1483A, Scale 1 : 50 000*, Geological Survey of Canada: Ottawa.
- Quinn PF, Beven KJ, Chevallier P, Planchon O. 1991. The prediction of hillslope flowpaths for distributed modelling using digital terrain models. *Hydrological Processes* **5**: 59–80.
- Reutebuch S, McGaughey RJ, Andersen HE, Carson WW. 2003. Accuracy of a high-resolution LiDAR terrain model under a conifer forest canopy. *Canadian Journal of Remote Sensing* **29**: 527–535.
- Roy JW, Hayashi M. 2008. Groundwater exchange with two small alpine lakes in the Canadian Rockies. *Hydrological Processes* **22**: 2838–2846.
- Seibert J, McGlynn BL. 2007. A new triangular multiple flow direction algorithm for computing upslope areas from gridded digital

- elevation models. *Water Resources Research* **43**: W04501, DOI: 10.1029/2006WR005128.
- Smith SL, Holland DA, Longley PA. 2004. *The importance of understanding error in LiDAR elevation models*. 20th ISPRS conference. Istanbul, Turkey, 12–23 July 2004. Paper 488.
- Soenen SA, Peddle DR, Coburn CA, Hall RJ, Hall FG. 2008. Improved topographic correction of forest image data using a 3-D canopy reflectance model in multiple forward mode. *International Journal of Remote Sensing* **29**(4): 1007–1027. DOI: 10.1080/01431160701311333.
- Strahler AN. 1957. Quantitative analysis of watershed geomorphology. *American Geophysical Union Transactions* **38**: 913–920.
- Tarboton DG. 1997. A new method for the determination of flow directions and upslope areas in grid digital elevation models. *Water Resources Research* **33**(2): 309–319.
- Töyrä J, Pietroniro A, Hopkinson C, Kalbfleisch W. 2003. Assessment of Airborne Scanning Laser Altimetry (LiDAR) in a deltaic wetland environment. *Canadian Journal of Remote Sensing* **29**(6): 718–729.
- Tsukamoto Y, Ohta T, Noguchi H. 1982. Hydrological and geomorphological studies of debris slides on forested hillslopes in Japan. In *Recent Developments in the Explanation and Prediction of Erosion and Sediment Yield*. IAHS Publication 13; 89–98.
- Wahba G. 1990. *Spline Models for Observational Data*. CBMS-NSF Regional Conference Series in Applied Mathematics 59. SIAM: Philadelphia, PA.
- Wechsler SP. 2007. Uncertainties associated with digital elevation models for hydrologic applications: a review. *Hydrology and Earth System Science* **11**: 1481–1500.
- Winstral A, Marks D. 2002. Simulating wind fields and snow redistribution using terrain-based parameters to model snow accumulation and melt over a semi-arid mountain catchment. *Hydrological Processes* **16**: 3585–3603.
- Young GJ. 1991. Hydrological interactions in the Mistaya Basin, Alberta, Canada. In *Snow, Hydrology and Forests in High Alpine Areas*. International Association of Hydrological Sciences Publication: Vol. 205; 237–244.
- Zappa M, Pos F, Strasser U, Warmerdam P, Gurtz J. 2003. Seasonal water balance of an alpine catchment as evaluated by different methods for spatially distributed snowmelt modelling. *Nordic Hydrology* **34**: 179–202.